Denudation history of the continental margin of western peninsular India since the early Mesozoic – reconciling apatite fission-track data with geomorphology[☆]

Y. Gunnell [a,*], K. Gallagher [b], A. Carter [c], M. Widdowson [d], A.J. Hurford [e]

[a] Laboratoire de Géographie Physique, CNRS-UMR 8591, and Département de Géographie, Université de Paris 7, Case 7001, 2 Place Jussieu, 75251 Paris Cedex 05, France
[b] Department of Earth Science and Engineering, Imperial College London, South Kensington, London SW7 2AS, UK
[c] London Fission Track Research Group, Research School of Geological Sciences, Birkbeck College, Gower Street, London WC1E 6BT, UK
[d] Department of Earth Sciences, The Open University, Walton Hall, Milton Keynes MK7 6AA, UK
[e] Department of Geological Sciences, University College London, Gower Street, London WC1E 6BT, UK

Abstract

A comprehensive apatite fission-track (AFT) study of the passive margin of western peninsular India between 12° and 16°N is used to reconstruct the denudation chronology of the continental hinterland. In common with other rifted margins, the morphology is characterised by a low-lying coastal plateau separated from an elevated inland plateau by an erosionally controlled escarpment (Western Ghats). We modelled the fission track data using the commonly adopted annealing algorithm of Laslett et al. [Chem. Geol. 65 (1987) 1–13]. Using the default parametrisation (i.e. an initial track length of 16.3 μm), it was found that during the Mesozoic denudation rates remained extremely low, increasing sporadically when erosion peaked at 130 Ma (rifting with Antarctica) and 80 Ma (rifting with Madagascar). Denudation rates rose considerably during the Cenozoic, reaching maxima of ca 120 m/Myr. Such values are, however, considered as major overestimates and the effects of the Seychelles rifting at 65 Ma remain suspiciously unrecorded. We explored the consequences of changing the initial track length in this model to a value of 14.5 μm. In practice, this reduces the rapid Cenozoic denudation artefact, model peak rates during the Mesozoic are much more variable, and during the Cenozoic reach values an order of magnitude lower than with the original initial track length. The response to the Seychelles rifting event is almost immediate. Just as previous model calibrations in AFT analysis have been relatively empirical, this revised approach does not provide insights into the physical mechanisms of low-temperature annealing. However, it is shown to agree much better with independently established geomorphic, cosmogenic, stratigraphic and tectono-magmatic evidence in this and other stable shield regions in terms

* Corresponding author. Present address: Laboratoire de Géographie Physique, CNRS-UMR 8591, Campus du CNRS, 1 Place Aristide Briand, 92190 Meudon, France. Fax: +33-1-46-64-78-81.
  E-mail addresses: gunnell@paris7.jussieu.fr (Y. Gunnell), k.l.gallagher@ic.ac.uk (K. Gallagher), a.carter@ucl.ac.uk (A. Carter), m.widdowson@open.ac.uk (M. Widdowson), t.hurford@ucl.ac.uk (A.J. Hurford).

of both the timing and the magnitude of geological events, and the geomorphic response of the landscape to them.

1. Introduction

Passive margins constitute about half of the overall length of present-day continental coastlines and represent the transition between the relatively simple tectonics of the oceans and the more complex settings of continents. Onshore morphologies at mature passive margins are mostly controlled by the denudation-related unloading onshore, the magnitude and spatial distribution of the sediment load offshore, and the lithospheric strength across the margin (i.e. isostatic rebound) [1,2]. As it is primarily the post-rift denudational history that regulates the nature and timing of sediment supply to the offshore margin, an understanding of the long-term onshore evolution of these margins is of fundamental importance to passive margin models.

Previous studies have used apatite fission-track (AFT) data to quantify the degree, rate, and timing of denudation in a selection of passive margin settings (e.g. [1,3–7]). To varying degrees, these studies also considered the wider consequences of the inferred denudation chronology in terms of the evolution of passive margin topography. AFT is particularly suited to the problem of resolving depths of post-rift denudation on the scale of < 5 km. This is a consequence of the sensitivity of annealing of fission tracks in apatite to temperatures up to 120°C on timescales of 1–100 Myr. Moreover, the technique is ideal in areas such as the Indian shield, which onshore is largely devoid of direct post-rift chronostratigraphic indicators.

On the basis of extensive new AFT analyses and integrated geomorphological data, this contribution aims to provide a quantitative overview of long-term denudation at the western Indian margin, and to infer the morphotectonic evolution of the Western Ghats. To achieve this it is necessary to (i) quantify the cooling history recorded in the AFT data and (ii) infer regional denudation rates that are compatible not only with AFT data,

but with other chronostratigraphic and geomorphological evidence.

2. Regional tectonic, physiographic and geological setting

Here we briefly summarise the geological and geomorphological evolution of the western India passive margin. More detail is available in previously published work [8]. Since the early Mesozoic, peninsular India has been involved in major rifting events related to the break-up and subsequent dispersal of eastern Gondwana, which began during the latest early Jurassic (ca 180 Ma; [9]). This was followed at ca 130–120 Ma by the separation of a fragment incorporating India and Madagascar from eastern Africa to the west, and from Antarctica to the east. The formation of the present western Indian margin was effected by the late Cretaceous separation from Madagascar (ca 88 Ma; [10]) and, finally, by a ridge-jump which detached India from the Seychelles Bank at the time of the Deccan continental flood basalt (CFB) (ca 65 Ma; [11]).

The onshore topography of India's western margin displays many features that are characteristic of other rifted margins [8] and, in particular, the morphological succession from the coast to the continental interior. In the study area (Fig. 1), these are from west to east: (i) a low-lying coastal plateau (the Konkan–Kanara lowlands) with short, seaward-flowing rivers; (ii) a coast-parallel, continental-scale escarpment with relief ranging between 0.6 and 2.2 km at a distance of 0–70 km inland of the present-day coastline; and (iii) an elevated inland plateau (Karnataka and Maharashtra uplands). The escarpment currently forms, with a few exceptions involving drainage piracy, the main drainage divide of peninsular India: eastward-draining rivers rise often within 50 km of the Arabian Sea, yet discharge into
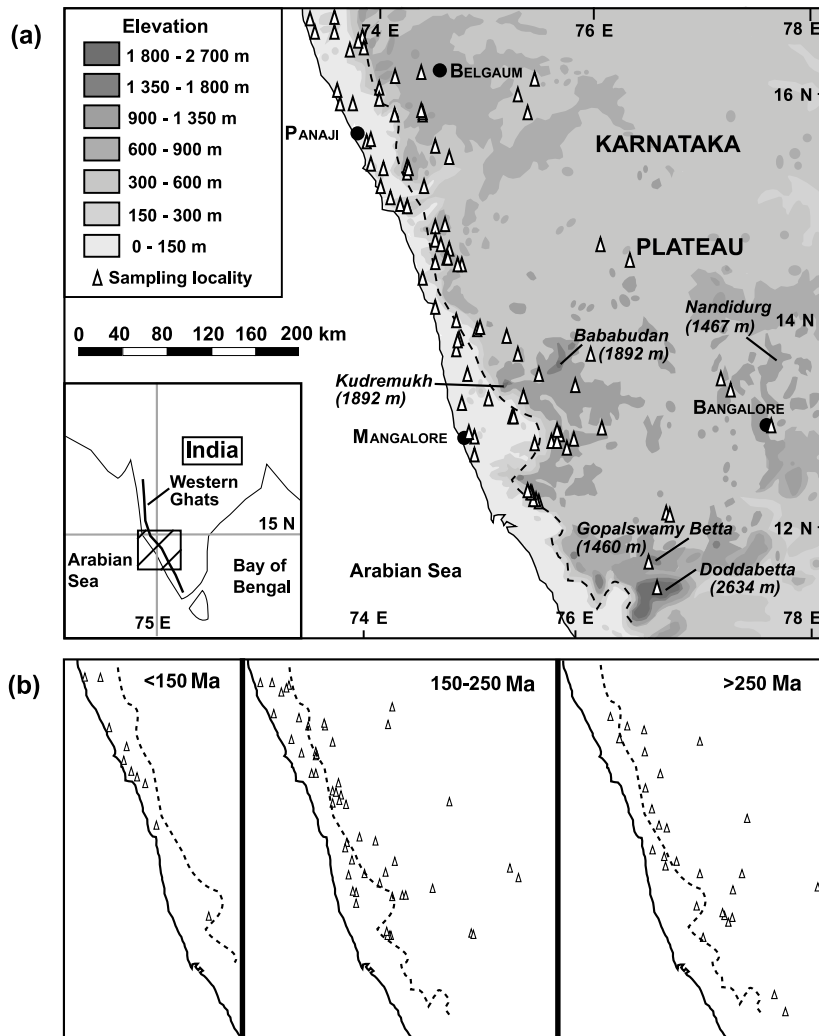
Fig. 1. Onshore topography of the western Indian margin and distribution of apatite samples. Dashed line marks the topographic division (panel a) used for the 'lowland' and 'upland' provinces discussed in this paper. (b) Detailed geographical distribution of apparent AFT ages, revealing that the pattern across the two defined provinces is complex for ages >150 Ma.

the Bay of Bengal. The well-defined Western Ghats escarpment is only partly associated with surface volcanics in the north, while the geology of the southern part is Precambrian basement. Thus, while the surface uplift may reflect mantle processes (e.g. the influence of a plume or hotspot), the surface expression of this potential contribution is geographically restricted.

Fig. 2 shows a simplified geological map of the region featuring the near-flat-lying late Cretaceous to early Tertiary CFB and the Precambrian

gneiss and greenstone basement complex onto which the lavas were extruded (Dharwar craton). The CFB provides the main regional chronostratigraphic marker by reference to which the subsequent morphotectonic development of the margin can be reconstructed. A gentle seaward-dipping monocline lying 10–30 km seaward of the Western Ghats escarpment has been inferred from stratigraphical and structural studies of the Deccan lava succession. This has been interpreted as a post-eruptive but undated modification resulting
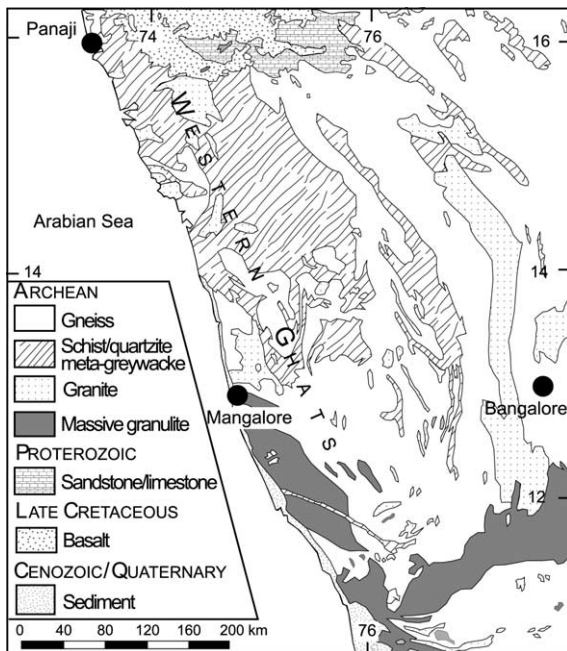
Fig. 2. Geology of the Dharwar craton, SW India.

from localised uplift of the lavas [12]. A number of fault lines, however, have also been identified in the onshore coastal zone, in addition to the well-known Panvel flexure near Bombay, so that it has also been argued that the monocline in the basalts is a syn-eruptive roll-over structure [13]. The faults, however, do not currently define relief features and the monocline, whether syn-rift and structural or post-rift and flexural, has been fairly uniformly breached by the receding drainage systems. The current escarpment is thus primarily an erosional feature [8].

3. AFT data

3.1. Sampling and analytical procedures

A suite of 128 samples was collected across major topographic variations at the western Indian margin between 10° and ca 16°N (Fig. 1), and analyses for 92 of these are reported here. The main limits to sampling further north were the Deccan CFBs, which do not contain sufficient

apatite for analysis. In addition, the Archean greenstone rocks forming the higher summits (ca 1.9 km) of the Ghats and the plateau also tend to comprise unsuitable lithologies. This restricted sampling from the higher elevations of the craton, but auxiliary geomorphological evidence aided the interpretation of the denudation chronology in these localities.

Apatite was separated using conventional crushing, sieving, heavy liquids and magnetic techniques. Apatite crystals 80–500 μm in size were polished and etched using HNO_3 5M at $20 \pm 1°C$ for 20 s, while low uranium muscovite, used as an external detector [14], was etched using 48% HF for 50 min. Samples were irradiated at the well-thermalised Risø reactor in Denmark, using the Corning CN5 glass dosimeter. Analyses were carried out on a Zeiss Axioplan microscope at a magnification of $\times 1250$, using a dry ($\times 100$) objective. Confined track length measurements were made using a drawing tube and digitising tablet, calibrated against a stage micrometer. Fission-track ages (Table 1) were calculated using the ζ calibration approach [15], as recommended by the I.U.G.S. Subcommission on Geochronology [16].

3.2. Qualitative discussion of AFT data

The major recent tectonic event in western India was rifting and CFB magmatism around 65 Ma. The relationship between the AFT age and the mean track length (MTL) is a useful way to identify discrete thermal events in a given region [1,17,18]. If the data form a coherent boomerang-shaped trend, then they may be interpreted in terms of a discrete cooling event with differential cooling, such that the oldest samples experienced the least cooling and the youngest the most. Provided the youngest samples have MTLs $> 13.5–14$ μm, then the AFT age approximates the timing of the cooling event, otherwise it provides an upper limit to this timing. Fig. 3 shows the relationship between the AFT age and the MTL for the data from western India.

The youngest ages are 55–75 Ma. The corresponding samples have relatively long MTLs (≥ 13.5 μm) and are geographically close to the
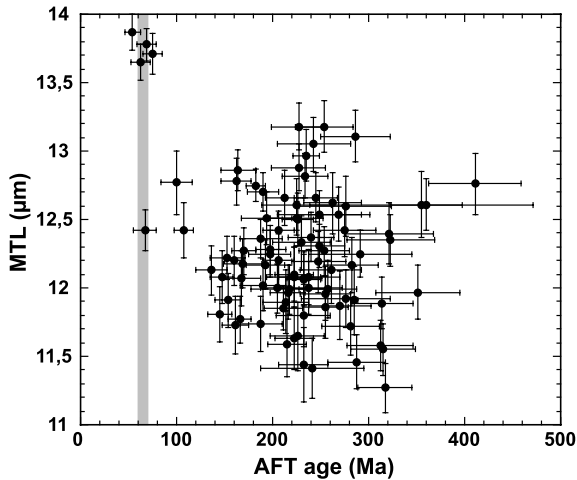
Fig. 3. Relationship between AFT age and mean confined track length (MTL). Error bars are 2σ and vertical grey band indicates the time of rifting related to the Deccan CFB. The scatter and moderately short MTL for a majority of samples indicate a complex cooling history.

present-day outcrop of the Deccan CFB, in the north of our study area. The other samples with young AFT ages generally have MTLs < 13 μm, and these were collected at much greater distance from the Deccan CFB. The majority of the samples have AFT central ages ranging from 150 to 300 Ma and MTLs between 11.5 and 13 μm. These data indicate variable amounts of cooling and thus do not conform to the simple trend of a single cooling event related to a change in regional heat flow as might be expected during the formation of a volcanic margin such as this.

3.3. Geographical variation

Previous studies of other passive margins have indicated an important geographical control on cooling (and so AFT age and MTL) in terms of the position of the sampling localities within the coastal plain–escarpment–inland plateau morphological units [1,3,4]. Given that elevation tends to vary systematically with position from the rift axis or the present-day coast towards the continental interior, there is often a correlation between elevation and the AFT age. The AFT ages from western India have a tendency to increase with elevation (Fig. 4), with the oldest ages being ob-

tained from the highest summits sampled (IND2308, 1450 m: 351 ± 22 Ma; and IND2305, 2630 m: 411 ± 24 Ma). However, although relatively young ages are exclusively associated with samples from low elevations (e.g. no age < 150 Ma is found above 400 m), some samples from the low-lying coastal zone yield relatively old ages. This observation is not exceptional in comparison with other known high-elevation passive margins, where a clear-cut younging of ages is not always observed (e.g. SW Africa, SE Australia) between the upland interior and the coastal plain [1,18]. In summary, the Western Ghats escarpment separates two AFT age groups: one with ages typically greater than 220 ± 10 Ma (i.e. in the upland plateau, with elevations generally > 400 m), and one with ages lower than 220 ± 10 Ma (i.e. in the coastal lowland). However, this division does not simply reflect a progressive younging of ages from the continental interior towards the coast. In detail, the pattern is clearly more complex.

The northernmost samples, close to the present outcrop of the Deccan CFB, have the youngest ages and also show the longest MTLs, implying that they record a relatively discrete cooling event. Given that, within error, the AFT ages between 54 and 72 Ma correlate with the Deccan CFB episode (65 Ma), this suggests a thermal event related to the formation of the Deccan CFB. However, as these samples are immediately surrounded by other samples at similar elevations with AFT ages three times greater, the localised
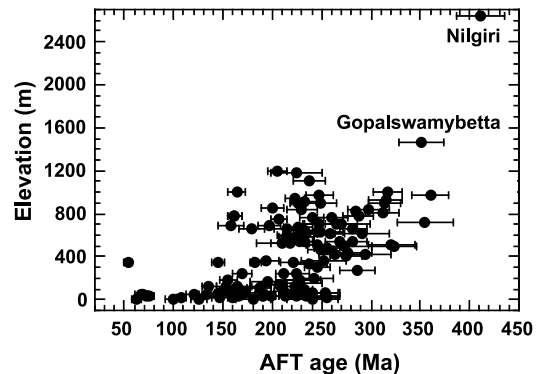

Fig. 4. Relationship between AFT age and elevation across the Dharwar craton.

nature effectively rules out heating by a large sub-lithosphere heat source (e.g. the Deccan source plume). An alternative interpretation of these young AFT ages is that reheating, followed by rapid cooling, is the result of burial of the Precambrian basement by a now eroded lava pile. A similar inference has been made for data from the Paraná CFB province in southeast Brazil [4] and, given the relatively low thermal conductivity of basalt (e.g. between 1.59 and 1.85 W m^{-1} K^{-1} for the Deccan basalt [19]), would imply between 2 and 4 km of burial to achieve total annealing. Again, however, the localised nature of these few samples is problematic. The chemistry of these apatites was also considered as a possible factor of deviation from the regional trend, but a comparative microprobe analysis of those samples and others (older ages and/or different elevations) from the same area revealed identical geochemical signatures (IND2033, 69 ± 5 Ma: mean F 2.82 wt% and mean Cl 0.01 wt% based on 16 grains; IND2030, 160 ± 10 Ma: mean F 2.29 wt% and mean Cl 0.04 wt% based on 15 grains; IND2000, 245 ± 11 Ma: mean F 2.05 wt% and mean Cl 0.03 wt% based on 30 grains). Consequently, we suggest that these samples most likely represent local resetting due to either local lava flows or late minor intrusions [20], which are common along the coast but not easily identified because of generalised deep lateritic weathering. If reheating was caused by local lava flows, it implies that those samples must have been close to the pre-eruption surface as the thermal effects of lava flows occur over a similar length scale to individual flow thickness [4]. In either case, the inferred cooling for these few samples is not solely attributable to denudation.

4. A quantitative denudation chronology of the Western Ghats margin

4.1. Thermal history modelling assumptions and procedure

To obtain quantitative thermal and denudation histories for the large sample population, we followed the procedures described by Gallagher [21] and Brown et al. [6]. The thermal modelling uses a guided search (genetic algorithm) combined with a maximum likelihood criterion to identify thermal histories, optimal in terms of fitting the observed track counts and length data. Each sample was modelled independently, although the same parameter space was used to define the range for temperature and time values. In this study we use the algorithm designed by Laslett et al. [22] to simulate the temperature and time dependence of fission-track annealing in apatite. It is an empirical model, calibrated against an extensive series of laboratory annealing experiments. Currently, it is probably the most commonly adopted annealing algorithm and is generally applicable to the more common compositions of apatite (i.e. similar to the Durango apatite age standard used to calibrate the model).

The original calibration [22] was based on fitting the empirical model to a transformation of the laboratory annealing data involving a normalisation of the measured sample track length l by an initial length l_0 in the unannealed apatite. One of the key assumptions in developing this calibration was that uncertainty around unannealed track lengths in apatite was negligible, with $l_0 = 16.3$ μm in the original model formulation. This initial length was calibrated from induced track length measurements. More recent work has shown that the initial length of induced tracks is perhaps 5% greater and that room temperature annealing occurs over timescales of a few weeks for induced tracks [23]. Furthermore, it also appears that geological samples that have remained at temperatures < 40°C have MTLs considerably shorter than predicted from the Laslett et al. annealing model [24,25]. Some of these samples, such as the Durango apatite, are used as age standards, whereby it is implicitly assumed that the level of annealing is minor. However, these 'unannealed' age standards have MTLs of 14.5–15 μm, implying that the effective initial track length for geological timescales and spontaneous tracks may be ∼ 10% lower than that observed on laboratory timescales with induced tracks [26–28]. The consequence of these observations is that the Laslett et al. model, as originally formulated, appears not to predict sufficient amounts of anneal-

ing at temperatures lower than 50–60°C. In the context of inferring thermal histories from geological samples, this limitation often results in artificially generating a late cooling event, typically implying >1 km of recent denudation, to bridge the gap between the known surface sampling temperature and the significantly higher temperature required by the Laslett et al. model to account for the observed amount of annealing.

A definitive solution to this problem is not the aim of this paper, but in principle the issue can be approached from four directions: (i) designing new annealing algorithms based on independent experimental research [27], but with the problem of extrapolating laboratory experiments to geological timescales; (ii) calibrating estimated depths of denudation against independent chronostratigraphic and geomorphic data [29,30], but with implicit uncertainty in the underpinning geomorphic theories; (iii) performing cross-calibrations of AFT data against other radiometric techniques, but with the risk of having to face uncertainties inherent in the physical underpinnings of several, rather than just one, technique [31]; (iv) exploring new parametrisations of existing AFT annealing algorithms.

In this paper we follow the latter approach, in that we consider the consequences of adopting an initial track length of 14.5 μm in addition to using the conventional value of 16.3 μm. We recognise that, as such, this approach does not directly provide new insights into the physical mechanisms of low-temperature annealing, and this is not our aim. However, other existing model calibrations are themselves relatively empirical [26,27], and the entire philosophy behind thermochronology based on age standards derives precisely from the elusiveness of some key physical underpinnings [15]. Furthermore, other annealing models sensitive to our concerns about low-temperature annealing, and therefore potentially suited to comparisons with our own approach (e.g. [27]), are based on a different laboratory protocol to that used by both Laslett et al. and by us; also, the statistical procedures used in the model calibration have been questioned [32]. The motivation for our approach is that, by modifying a single parameter within an otherwise well-known model,

we explore the artefacts associated with the initial model relative to shorter MTL annealing, and thus compare the denudation chronology results with independent chronostratigraphic data [8] in order to assess the geological viability of the model results.

Having obtained an optimal data-fitting thermal history for each sample independently, we need to convert the temperature histories to corresponding depths of denudation. We do this using the following form of Fourier's law for heat conduction:

$$z = (T(z) - T_s)\frac{k}{Q} \qquad (1)$$

where z is depth, $T(z)$ is temperature at that depth (obtained from modelling the AFT data), T_s is the surface temperature, k is the average thermal conductivity of the rock down to depth z, and Q is the surface heat flow. Across the Dharwar craton, the present-day temperature gradients and heat flow are fairly low and homogeneous, 11–15°C km^{-1} and 35–40 mW m^{-2}, respectively [33–35]. Such low values are not unusual for stable cratonic shields, and as the craton is not known to have experienced significant thermal disturbances since at least the Pan-African orogeny, we adopt a spatially constant heat flow of 40 mW m^{-2} across the region. We assumed a thermal conductivity of 3.25 W m^{-1} K^{-1} for the eroded crustal section, based on reported values for the Dharwar craton [19,35] and a constant surface temperature of 20°C. The resulting geothermal gradient is also constant, and equal to 12.3°C km^{-1}.

We also considered the influence of heat flow variations over time (assuming an exponential decay with time since continental break-up), and also the effect of changing the thermal conductivity (by ±50%). The absolute values of the denudation rate varied in a predictable way from Eq. 1. Thus, increasing Q leads to a decrease in equivalent denudation depth, while increasing k leads to an increase in equivalent depth. We do not show the results here, but the relative variations in the denuation chronology over time were maintained (i.e. the peaks were still peaks). Thus, we consider the features in the denudation chronologies we show later to be robust to the adopted

thermal parameters, particularly rift-related heat flow, which after an initial increase tends to decrease slowly with a time constant of about 60 Myr, i.e. longer than the timescale of the variations inferred here.

To quantify the regional denudation chronology, we interpolate the results for each sample using a nearest-neighbour approach [36], and then spatially integrate the denudation estimates over a specified area at discrete time intervals. By doing this at 1 Myr intervals and dividing by the area over which the integration was made, we obtain an estimate of the average denudation rate as a function of time for that specific area. As shown in Fig. 1, the geographical spread of apatite samples is not evenly distributed. To assess the introduction of potentially spurious features as a consequence of the interpolation procedure, we have also calculated the mean denudation rate from the individual cooling histories (i.e. without spatial interpolation). The interpolation procedure does satisfy the data exactly at each sample point, but the interpolation between data can lead to some samples having an undue influence on the spatial integration. We also determined the weighted mean denudation chronology, where the weights were the uncertainties on the temperatures in the thermal history for each individual sample. As a guide to the uncertainty on these average denudation chronologies, we calculated the standard error on the weighted mean values, σ_{wm} using the following formula:

$$\sigma_{wm}^2 = \left(\sum_{i=1}^{N} \frac{1}{\sigma_i^2} \right)^{-1} \qquad (2)$$

where σ_i is the uncertainty on an individual thermal history at a given time, and N is the total number of thermal histories. These calculated uncertainties are considered indicative of the magnitude of the minimum uncertainty inherent in the spatially interpolated curves. The aim of this is to examine which features in the denudation chronology are robust to the interpolation and integration procedure, and to the errors in the thermal histories (i.e. which features appear in all three curves).

We present the results of this analysis for two sub-areas of the study region, chosen for their morphotectonic setting. These are referred to as the 'upland' and 'lowland' provinces, and effectively represent the regions seaward and landward of the present-day escarpment (Fig. 1). The relative variations between the denudation chronology curves calculated in the way described above are such that the spatially averaged denudation rate curves (heavy black line) are representative of the general patterns for these two areas. For interpretation purposes, the spatially averaged 'upland' and 'lowland' curves have therefore been preferred in this study unless otherwise stated. The major differences in the interpretation options lie between the two AFT calibrations considered.

4.2. Denudation chronology of the Indian rifted continental margin

4.2.1. Results with an initial track length of 16.3 μm

In Fig. 5a,b we show the smoothed denudation chronologies for the upland (16up) and lowland (16lo) areas using the thermal histories derived with the Laslett et al. Durango apatite annealing algorithm [22], using an initial track length of 16.3 μm. The smoothing is a simple 10-point running average, and serves to incorporate the fact that the timing of cooling events has an inherent uncertainty in addition to the uncertainty on the temperatures. It is thus also a cautionary measure that we advocate to avoid over-interpreting the significance of sharp peaks in the raw data curve. For the spatially interpolated denudation curves, both regions show distinct peaks of enhanced denudation marking the rifting events of both the east (Antarctica, ca 120 Ma) and the west coasts (Madagascar, ca 80 Ma; Seychelles, ca 65 Ma) of India, although the peak for the latter is relatively subdued or smeared into the 80 Ma peak.

Overall, this sequence of events is consistent with denudation chronologies of peninsular India based on geomorphology and basin analysis [8], although the inferred denudation peak at 80 Ma cannot be correlated in detail with offshore sedimentary sequences because existing offshore oil
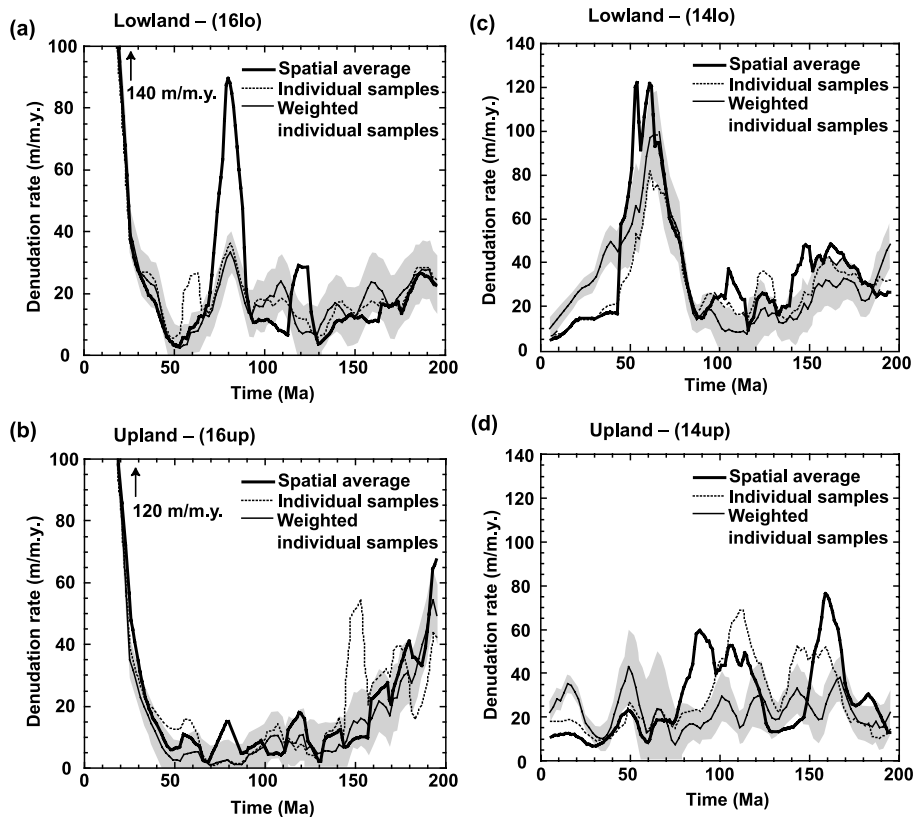
Fig. 5. A comparison of AFT denudation curves for the lowland and upland areas based on (a,b) initial track lengths of 16.3 μm; and (c,d) 14.5 μm (rounded-off appellations of 16lo and 14lo are meant to emphasise that we are exploring upper and lower end-member values of initial track length rather than any precise value). The lowland samples are the sub-population of samples located seaward of the Western Ghats escarpment (see Fig. 1). The spatial average (thick solid line) is based on interpolating the results over each sub-area; the individual sample curve (dashed line) is the unweighted mean of the denudation chronology at individual locations; the weighted sample curve (thin solid line) is the mean denudation at individual locations, weighted by the uncertainty in the inferred thermal history for each location. The shaded area is the standard error on the weighted mean estimate and is considered to indicate the magnitude of uncertainty inhererent in the modelling procedure.

wells only currently reach the bottom of the Cenozoic, post-rift sediment pile. The denudation chronologies calculated without the interpolation also have the inferred peak around 80 Ma in the lowland province but not in the highland region. In addition, the timing of the earlier (120 Ma) peak is a little later, occurring around 110–100 Ma. Thus, all three methods involved in calculating an average denudation rate chronology imply enhanced denudation around 80 Ma in the lowland area, and a major increase starting around 70–50 Ma and lasting to the present day.

In terms of timing, the sharp increase in denudation recorded during the Neogene is problematic. The AFT rates of accelerated denudation in the Cenozoic borne out by the 16lo curve (Fig. 6a) result in over-supplying the offshore basins when compared with the limited data on the sediment volumes effectively detected offshore [37]. We suggest that this overestimate may be partially attributable to the 16.3 μm initial track length adopted in the annealing model [22], which tends to underestimate track annealing at sub-60°C temperatures, and therefore to overestimate total cooling rates in the more recent geological past. Additionally, it may of course be a reflection of sediment transport out of the system either as detrital material or dissolved load, but existing

offshore data provide few high-resolution constraints on this issue.

4.2.2. Results with an initial track length of 14.5 μm

In Fig. 5c,d, we show smoothed denudation curves for the upland (14up) and lowland (14lo), where we adopted an initial track length of 14.5 μm. There are few similarities between these results and those obtained from the 16.3 μm value. Here, (i) during the Mesozoic (200–100 Ma), conspicuous denudation peaks in the highland area, i.e. that closest to the eastern margin of India, reflect high denudation rates in response to the onset of rifting of Gondwana around 170 Ma [9]. The products of this episode are to be found in the thick clastic fills of the early Jurassic rifts and aulacogens along the eastern margin of India. Denudation resumed at ca 120 Ma, as a response to the rifting-apart of Antarctica and Greater India. Clearly, denudation related to base-level changes in the Bay of Bengal significantly affected the current Western Ghats region, which lies ca 800 km from the eastern seaboard, suggesting that the denudation signal reached far into the interior of Greater India via an easterly peninsular drainage already in existence at the time. (ii) The current lowland area shows a sharp rise in denudation rates (ca 120 m/Myr) during the late Cretaceous (80–70 Ma: Madagascar rifting), also apparent though more subdued (ca 60 m/Myr) in the upland area. (iii) In the coastal zone, the major denudation event at 80–70 Ma merges with the Seychelles rifting event at 65 Ma before denudation rates definitively decline after 50 Ma. In the uplands, this event forms only a secondary peak (ca 20 m/Myr) at 50 Ma, which is occulted in the adjacent lowland region by the much larger denudation peak occurring at that time (Fig. 6b). Increased erosion in middle Eocene times inferred from the Bombay offshore stratigraphic record has been attributed to a variety of triggering phenomena involving far-field lithospheric stresses (e.g. acceleration of hotspot ridge-push [38]); short-lived excess melting when the Réunion plume is understood to have crossed the Central Indian Ridge at 53–48 Ma [39]; or the long-range impact of the so-called 'soft' Himalayan collision

[40]. Although the AFT data cannot discriminate between these various causative mechanisms, we suggest here that the denudation recorded at the coast may simply reflect a delayed response to the Seychelles rifting of drainage basins eroding the plateau edge from the west. (iv) During the late Cenozoic, denudation curves for the sub-populations of samples collected respectively landward and seaward of the Ghats escarpment are similarly low in magnitude (5–15 m/Myr) and indicate a significant fall in denudation rates. The slight fall in rates after 20 Ma in the lowland zone (Fig. 5c) suggests that the coastal belt had become a base-level plain by that time. The low-relief, low-estuarine river gradients, and the penetration of ocean tides sometimes as far as the foot of the great escarpment is consistent with this. The slight rise in rates during that same time interval in the upland region (Fig. 5d) may reflect increased erosion caused by drainage piracy by west-flowing rivers receding into the plateau at the Western Ghats escarpment. Deranged drainage, reflective of recent river capture, is generalised between 13 and 15°N latitude [8].

In summary, from the comparison between the 16 and 14 curves of Fig. 5, the most significant differences arise clearly from the underlying differences in the two model calibrations. These differences concern the timing of events, but most of all the magnitude of denudation: (i) the start of enhanced denudation during the Cenozoic occurs earlier for the shorter intial track length and correlates with the time of rifting from Madagascar followed by the Seychelles, while the longer initial track length does not bring out the Seychelles rifting event and implies a delay of about 20 Myr after it. (ii) The results also imply that, although the Cenozoic denudation chronologies of the highland and lowland areas are very similar within each modelling protocol, suggesting that each approach is internally consistent, the maximum Cenozoic denudation rates differ by an order of magnitude.

5. Discussion

The Cenozoic denudation patterns are the most

relevant to understanding the morphology of the present-day Indian landscape. Here we focus on the contrast in denudation patterns offered by the two model parametrisations presented above, and examine these in the light of independent geological and geomorphological data.

5.1. Denudation in the uplands

The original annealing model calibration (16up, Fig. 5a) implies that > 4 km of crustal material was removed from the upland region during the Cenozoic (since ca 50 Ma). Denudation rates rose to ca 120 m/Myr, i.e. roughly an order of magnitude more than in the Mesozoic. In contrast, the shorter initial track length (14up, Fig. 5c) implies < 1 km of mean Cenozoic denudation since 50 Ma. This depth of denudation is closer to that inferred from the relief between the current mean elevation of the Karnataka plateau surface
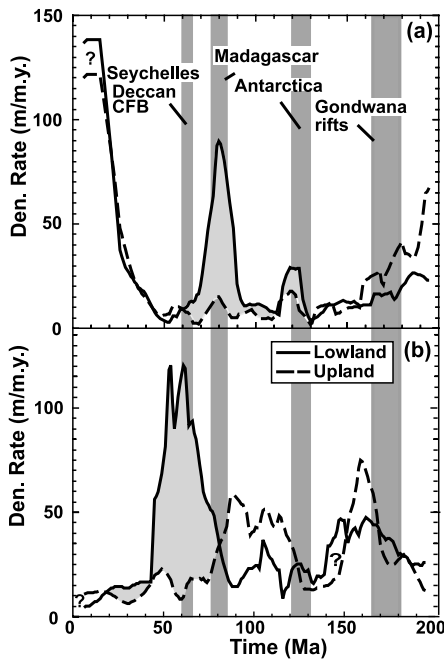

Fig. 6. Summary of denudation histories in the Western Ghats region according to (a) the conventional [22] and (b) our revised approaches. Shaded areas indicate the differential between denudation rates landward and seaward of the Ghats escarpment. Shaded bars indicate the known rifting events at both Indian passive margins during the break-up of Gondwana.

(0.6–0.9 km) and the many residual bedrock summits encountered on the plateau (ca 1.9 km). Although such topographic differences are no accurate measure per se of effective depths of denudation because residual bedrock landforms are also likely to have a history of surface denudation, there is growing evidence from Australia and West Africa, supported by multiple chronometric studies [31,41], that long-term erosion of bedrock and laterite summits is typically < 2 m/Myr. In substance, those studies reveal that depths of post-Mesozoic denudation in stable cratonic environments are not much greater than the currently observed residual differences in topography. Pending further cross-calibration of our Indian fission-track data with U–Th/He and cosmogenic nuclides (in progress) to verify this in greater detail, it may thus be tentatively inferred that the maximum observed relative relief on the Karnataka plateau is the result of differential erosion operating since the late Cretaceous between the resistant bedrock residuals and the more weatherable (and most widely sampled for apatite) tonalitic gneisses that now form the extensive upland plain.

5.2. Denudation in the coastal zone

Post-break-up denudation values are generally expected to be considerably higher across the coastal lowland and at the escarpment face of a rift than on the backslope [42]. The results of this study show that the largest signal of differential denudation between the upland and lowland provinces occurred at ca 100–80 Ma (Fig. 6a) or between 90 and 45 Ma, depending on the initial track length calibration being used. The overlap covering the rifting period between India and Madagascar is a sign that this was a major period of rift-flank denudation. Although the anticipated sedimentary products have not been encountered by offshore drilling exploration because current drilling depths only reach the roof of ca 65 Myr old basalt flows through post-rift sediments [8,37], this new evidence is the first indication so far provided that significant volumes of syn-rift, possibly petroleum-bearing sediment supplied by the Indian margin but sealed by the Deccan basalts may

lie offshore. The shorter initial track length model, however, also suggests that rapid denudation continued into the Palaeocene. This is confirmed by offshore terrigenous input recorded in exploration wells [37], a fact which brings out as suspect the occultation by the conventional model (Fig. 6a) of any rapid denudation occurring in response to post-Seychelles rifting.

During the Cenozoic, the curves show that denudation was either considerable (Fig. 6a), or relatively small (Fig. 6b), again depending on the parametrisation used. The very high rates (140 m/Myr) during the last 30 Myr as given by the 16.3 μm model are comparable to rates in active orogens and at odds with all other evidence in the region. The much lower Cenozoic rates afforded by the 14.5 μm model call for quite a different set of interpretations, with a possible analogue in SW Africa [1]. In contrast to previous models for the evolution of passive margin topography (e.g. [42]), where high estimated erosion rates in the coastal zone impose high differentials of denudation and therefore high magnitudes of flexural rebound, our results imply that relatively little modification of the topography occurred during later Cenozoic times: denudation in the lowlands was not significantly higher than in the uplands. In India, we tentatively interpret this situation as being a direct consequence of the relatively small size of the subcontinent. Unlike passive margins bounding vast, sometimes internally drained continental hinterlands, peninsular India is relatively narrow. The Karnataka uplands are externally drained towards the Bay of Bengal, which is situated 600–800 km from the Western Ghats headwaters. This configuration may be sufficient to explain the sensitivity of peninsular India to base-level changes (eustatic or otherwise), and hence the relatively high denudation rates (by cratonic standards) recorded landward of the escarpment. This may not be unique to India: the interiors of South Africa and Brazil also have a history of external drainage and denudation via the Orange and Paraná–São Francisco River basins, respectively, but because of its smaller scale the Indian setting is possibly a more simple example. In summary, the major differences arising from the competing models are that (i) escarp-

ment growth ceased at 40–20 Ma (14lo) instead of at 60 Ma (16lo); and (ii) the relatively long-term steady state of the escarpment after these respective dates was achieved in a context of exceedingly high rates on either side of it according to Fig. 6a, but much more reasonable and realistically fluctuating rates according to Fig. 6b.

6. Concluding statements

The AFT denudation chronologies described in this paper are as elsewhere model-dependent, both in terms of timing and magnitudes of denudation. In India, it appears that results derived with an initial track length of 14.5 μm provide closer agreement with existing geological data than those suggested by the more widely adopted Laslett et al. model with an initial track length of 16.3 μm. While the longer initial track length has been applied in earlier studies with no apparent problems (e.g. Brazil [4]), the inference of rapid, recent cooling when using the longer initial track length becomes most acute when dealing with data with relatively old AFT ages (> 200 Ma), with moderately short MTLs (e.g. 11–13 μm), which is typical of the data from India presented here. It appears logical to believe that this might reflect the nature of the data, i.e. when fission-track ages are younger, the spuriousness of the rapid cooling problem should be less acute. The generality of this point nevertheless demands to be tested in a suitably wide range of settings, as rapid recent cooling may in some cases be real (supported by independent geological evidence) rather than merely an algorithm-related artefact. It is important to clarify that the annealing models are empirical, based on fitting primarily laboratory timescale data, and subsequently extrapolating these results to geological timescales. Given these limitations, we believe the 14.5 μm model overall leads to geologically more robust conclusions about patterns of denudation for western India. We identify three main arguments in favour of this.

First, in terms of timing, one major difference between the 16.3 μm and the 14.5 μm models is the start of enhanced denudation after the main

late Cretaceous rifting and CFB event. The conventional model predicts a delay of about 20 Myr (Fig. 5a) before the denudation rate increases noticeably. In general, the time of increased denudation across a passive margin will be a reflection of the connectivity of the existing drainage systems with a potentially new base level, associated with rifting and continental break-up. It is difficult to explain in geomorphological terms such a 20 Myr hiatus seaward of the Western Ghats escarpment. The 16lo curve implies that rifting of the Seychelles plate at 65 Ma had no significant geomorphological effect upon the non-volcanic portion of the Western Ghats margin. However, if the 14lo curve (Fig. 5c) is considered, the increase in denudation rates is sustained throughout the period encompassing the close succession of established rifting events at 90–80 and 65 Ma (e.g. [10,11]). We conclude that the 14.5 μm model at least offers a more satisfactory fit to independent geological data than the more commonly adopted Laslett et al. [22] parametrisation with an initial track length of 16.3 μm.

Second, in terms of denudation magnitudes, major discrepancies are observed between the denudation peaks at successive intervals of the geomorphic history. Landward of the current Western Ghats escarpment, the 14.5 μm model implies pre-CFB denudation rates of ca 50 m/Myr. Such values appear to be justified for a small continent such as India, which has experienced rifting events in relatively close succession (e.g. with Antarctica only 40 Myr before it rifted from Madagascar). More strikingly, seaward of the escarpment, pre-CFB discrepancies between models are even more extreme, with about twice as much denudation at 90–80 Ma for 16lo relative to 14lo. The post-CFB period landward of the escarpment is where estimated rates between the two models diverge the most, i.e. by a maximum factor of 10–12. Seaward of the Western Ghats, the post-CFB denudation estimates also differ by the same factor.

The third and most compelling reason for preferring the shorter initial track length calibration is that it allows for differential denudation between the coastal and the upland regions during the Cenozoic as late as 20 Ma (shaded areas in Fig. 6b). In contrast, the conventional model calibration (Fig. 6a) implies that the Western Ghats escarpment is an extremely ancient landform, which developed during the peak of denudation at 100–80 Ma, was formed by 65 Ma, and has remained self-similar and in a steady state throughout the Cenozoic as denudation rates on either side of it remained identical. Irrespective of the denudation magnitudes involved, the notion of identical denudation rates on either side of the escarpment is quite obviously incompatible with the very existence of the escarpment itself as it also extends northward, where it is carved out of the Deccan Traps, which were not yet in existence at 80 Ma. The 14.5 μm model, in contrast, allows for (i) an even larger denudation differential (100 m/Myr) during the late Cretaceous, a proportion of which compensates the trend during the early Cretaceous when denudation in the current upland zone was higher than in the current coastal zone; followed by (ii) a continuation of higher rates into the late Eocene near the coast, after which denudation differentials diminish and probably only represent minor morphological adjustments. This fall in erosion rates after the pre-Eocene discharge of coarse clastic sequences into the offshore basin is in agreement with the known stratigraphy of the basin [8,37], with its >1 km thick Eocene to Middle Miocene limestone platforms reflecting low clastic input from the continent. Late to post-Miocene sediments consist of fine shale and clay, mostly reflecting the erosion of deep weathered mantles routed via the coastal rivers from the escarpment face and the plateau in relation to gorge recession and recent drainage piracies in the context of a highly aggressive monsoon climate [43].

In summary, until further progress in calibrating AFT annealing models is achieved, we suggest that the shorter initial track length model used in this study generates denudation curves that are in better agreement with geomorphic, stratigraphic and tectonomagmatic data than the conventional model calibration used in most previous AFT studies. We do not claim that this model is therefore better than the existing published models, but it does highlight the need for refining the latter through the incorporation of annealing data relevant to geological timescales. The quality and ap-

plicability of laboratory annealing models should further benefit from testing against independent constraints provided by well-understood natural settings, especially when AFT datasets such as this are geographically extensive and of a high analytical quality.

Acknowledgements

References

[1] K. Gallagher, R. Brown, The onshore record of passive margin evolution, J. Geol. Soc. Lond. 154 (1997) 451–457.

[2] Y. Gunnell, L. Fleitout, Morphotectonic evolution of the Western Ghats, India, in: M.A. Summerfield (Ed.), Geomorphology and Global Tectonics, Wiley, Chichester, 2000, pp. 321–338.

[3] T.A. Dumitru, K.C. Hill, D.A. Coyle, I.R. Duddy, D.A. Foster, A.J.W. Gleadow, P.F. Green, B.P. Kohn, G.M. Laslett, A.J. O'Sullivan, Fission track thermochronology: Application to continental rifting of south-eastern Australia, J. Aust. Petrol. Expl. Assoc. 31 (1991) 131–142.

[4] K. Gallagher, C. Hawkesworth, M. Mantovani, The denudation history of the onshore continental margin of S.E. Brazil inferred from fission track data, J. Geophys. Res. 99 (1994) 18117–18145.

[5] M.A. Menzies, K. Gallagher, A.J. Hurford, A. Yelland, Red Sea and Gulf of Aden rifted margins, Yemen denudational histories and margin evolution, Geochim. Cosmochim. Acta 61 (1997) 2511–2527.

[6] R. Brown, K. Gallagher, A.J. Gleadow, M. Summerfield, Morphotectonic evolution of the South Atlantic margins of Africa and South America, in: M.A. Summerfield (Ed.), Geomorphology and Global Tectonics, Wiley, 2000, pp. 255–281.

[7] S. Kalaswad, M.K. Roden, D.S. Miller, M. Morisawa, Evolution of the continental margin of western India: new evidence from apatite fission-track dating, J. Geol. 101 (1993) 667–673.

[8] Y. Gunnell, B.P. Radhakrishna (Eds.), Sahyadri, the Great Escarpment of the Indian Subcontinent. Patterns of Landscape Development in the Western Ghats, Geol. Soc. India Mem. 47, 2001, 1054 pp.

[9] M. Storey, The role of mantle plumes in continental breakup: case histories from Gondwanaland, Nature 377 (1995) 301–308.

[10] M. Storey, J.J. Mahoney, A.D. Saunders, R.A. Duncan, S.P. Kelley, M.F. Coffin, Timing of hot-spot related volcanism and the breakup of Madagascar and India, Science 267 (1995) 852–855.

[11] P.R. Hooper, The timing of crustal extension and the eruption of continental flood basalts, Nature 345 (1990) 246–249.

[12] M. Widdowson, K.G. Cox, Uplift and erosional history of the Deccan Traps, India: Evidence from laterites and drainage patterns of the Western Ghats and Konkan Coast, Earth Planet. Sci. Lett. 137 (1996) 57–69.

[13] H.C. Sheth, A reappraisal of the coastal Panvel flexure, Deccan Traps, as a listric-fault-controlled reverse drag structure, Tectonophysics 294 (1998) 143–149.

[14] A.J. Hurford, P.F. Green, A users' guide to fission track dating, Earth Planet. Sci. Lett. 59 (1982) 343–354.

[15] A.J. Hurford, Zeta: the ultimate solution to fission track analysis calibration or just an interim measure?, in: P. Van den Haute, F. de Corte (Eds.), Advances in Fission-Track Geochronology, Kluwer Academic, Dordrecht, 1998, pp. 19–32.

[16] A.J. Hurford, Standardization of fission track dating calibration: recommendation by the Fission Track Working Group of the I.U.G.S. Subcommission on Geochronology, Chem. Geol. 80 (1990) 171–178.

[17] R.W. Brown, M.A. Summerfield, A.J.W. Gleadow, Apatite fission track analysis: its potential for the estimation of denudation rates and implications for models of long-term landscape development, in: M.J. Kirkby (Ed.), Process Models and Theoretical Geomorphology, Wiley, Chichester, 1994, pp. 23–53.

[18] K. Gallagher, R.W. Brown, C.J. Johnson, Geological applications of fission track analysis, Annu. Rev. Earth Planet. Sci. 26 (1998) 519–572.

[19] F. Roy, R.U.M. Rao, Heat flow in the Indian shield, J. Geophys. Res. 105 (2000) 25587–25604.

[20] M. Widdowson, M.S. Pringle, O.A. Fernandez, A post K-T boundary (early Paleocene) age for Deccan-type feeder dykes, Goa, India, J. Petrol. 41 (2000) 1177–1194.

[21] K. Gallagher, Evolving temperature histories from apatite fission-track data, Earth Planet. Sci. Lett. 136 (1995) 421–435.

[22] G.M. Laslett, P.F. Green, I.R. Duddy, A.J.W. Gleadow, Thermal annealing of fission tracks in apatite, 2, A quantitative analysis, Chem. Geol. 65 (1987) 1–13.

[23] R.A. Donelick, M.K. Roden, J.D. Mooers, D.S. Carpenter, D.S. Miller, Etchable length reduction of induced fission tracks in apatite at room temperature ($\sim$23°C): crystallographic orientation effects and 'initial' mean lengths, Nucl. Tracks 17 (1990) 261–265.

[24] P. Vrolijk, R.A. Donelick, J. Queng, M. Cloos, Testing models of fission track annealing in apatite in a simple

thermal setting: site 800, leg 129, in: R. Larson, Y. Lancelot (Eds.), Proc. ODP Sci. Results 129 (1992) 169–176.

[25] J.D. Corrigan, Apatite fission-track analysis of Oligocene strata in South Texas, USA: Testing annealing models, Chem. Geol. 104 (1993) 227–249.

[26] G.M. Laslett, R. Galbraith, Statistical modelling of thermal annealing of fission tracks in apatite, Geochim. Cosmochim. Acta 60 (1996) 5117–5131.

[27] R.A. Ketcham, R.A. Donelick, W.D. Carlson, Variability of apatite fission-track annealing kinetics: III. Extrapolation to geological time scales, Am. Mineral. 84 (1999) 1235–1255.

[28] B.P. Kohn, A.J.W. Gleadow, R.W. Brown, K. Gallagher, P.B. O'Sullivan, D.A. Foster, Shaping the Australian crust over the last 300 million years: Insights from fission track thermotectonic imaging and denudation studies of key terranes, Aust. J. Earth Sci. 49 (2002) 697–717.

[29] M. Hill, Mesozoic regolith and palaeolandscape features in southeastern Australia: significance for interpretations of denudation and highland evolution, Aust. J. Earth Sci. 46 (1999) 217–232.

[30] Y. Gunnell, Apatite fission-track thermochronology: an overview of its potential and limitations in geomorphology, Basin Res. 12 (2000) 115–132.

[31] Y. Gunnell, Radiometric ages of laterites and constraints on long-term denudation rates in West Africa, Geology 31 (2003) 131–134.

[32] R.F. Galbraith, Some remarks on fission-track observational biases and crystallographic orientation effects, Am. Mineral. 87 (2002) 991–995.

[33] R.U.M. Rao, G.V. Rao, G.K. Reddy, Age dependence of continental heat flow - fantasy and facts, Earth Planet. Sci. Lett. 59 (1982) 288–302.

[34] M.L. Gupta, S.R Sharma, A. Sundar, Heat flow and lithospheric thickness of peninsular India, in: V. Cermak, L. Rybach (Eds.), Terrestrial Heat Flow and the Lithosphere Structure, Springer, Berlin, 1991, pp. 283–292.

[35] R.K. Verma, Geodynamics of the Indian Peninsula and the Indian Plate Margin, Oxford and IBH Publ. Co., New Delhi, 1991, 357 pp.

[36] M.S. Sambridge, J. Braun, H. McQueen, Geophysical prameterization and interpolation of irregular data using natural neighbours, Geophys. J. Int. 122 (1995) 837–857.

[37] N.K. Singh, N.K. Lal, Geology and petroleum prospects of the Konkan-Kerala basin, in: S.K. Biswas (Ed.), Proceedings of the Second Seminar on Petroliferous Basins of India, Indian Petroleum Publishers, Dehra Dun, 1993, pp. 461–469.

[38] M.H.P. Bott, Modelling the plate-driving mechanism, J. Geol. Soc. Lond. 150 (1993) 941–951.

[39] J. Besse, V. Courtillot, Paleogeographic maps of the continents bordering the Indian Ocean since the early Jurassic, J. Geophys. Res. 93 (1989) 11791–11808.

[40] M. Widdowson, C. Mitchell, Large-scale stratigraphical, structural and geomorphological constraints for earthquakes in the southern Deccan traps, India: the case for denudationally-driven seismicity, in: K.V. Subbarao (Ed.), Deccan Volcanic Province, Mem. Geol. Soc. India 43, 2000, pp. 425–452.

[41] P.R. Bierman, M. Caffee, Cosmogenic exposure and erosion history of Australian bedrock landforms, Geol. Soc. Am. Bull. 114 (2002) 787–803.

[42] A.R. Gilchrist, M.A. Summerfield, Tectonic models of passive margin evolution and their implications for theories of long-term landscape development, in: M.J. Kirkby (Ed.), Process Models and Theoretical Geomorphology, Wiley, Chichester, 1994, pp. 55–84.

[43] Y. Gunnell, Passive margin uplifts and their influence on climatic change and weathering patterns of tropical shield regions, Glob. Planet. Change 18 (1998) 47–57.